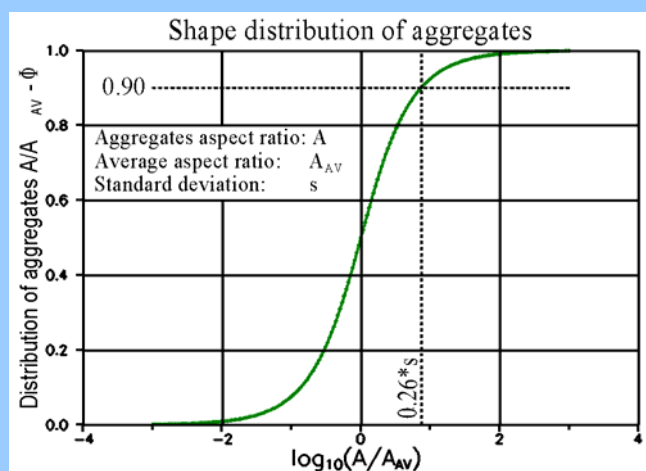
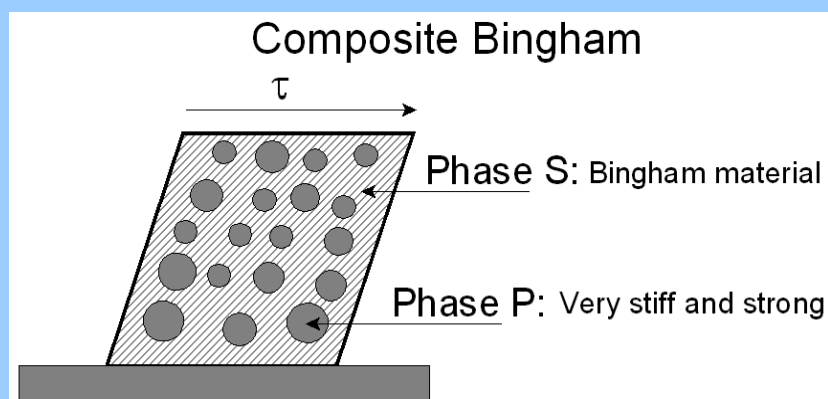
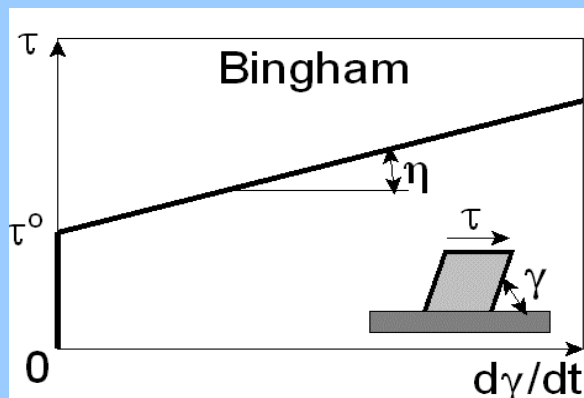


# A Bingham material mixed with stiff particles

## *some theoretical aspects*

Lauge Fuglsang Nielsen  
Department of Civil Engineering  
Technical University of Denmark  
DK-2800 Lyngby, Denmark



# **A Bingham material mixed with stiff particles**

## ***some theoretical aspects***

Lauge Fuglsang Nielsen  
Department of Civil Engineering  
Technical University of Denmark  
DK-2800 Lyngby, Denmark

### **CONTENTS**

1. INTRODUCTION.....	3
2. BINGHAM MATERIAL .....	3
3. COMPOSITE BINGHAM MATERIAL .....	4
Phase geometry and shape functions.....	4
Critical concentrations .....	5
Shape factors .....	6
Uni-shape mixture.....	6
Multi-shape mixture .....	6
4. COMPOSITE PROPERTIES.....	8
Viscosity.....	8
Yield stress.....	9
Pree-flow geometry .....	9
4. APPLICATION .....	10
Fresh concrete (SCC) versus mortar .....	10
5. FINAL REMARKS.....	11
6. NOTATIONS.....	11
APPENDIX A: Analogy .....	12
Elastic-viscous analogy.....	12
Elastic composite: shear modulus and phase stresses .....	12
Extremely stiff particles .....	12
Composite Bingham material: viscosity and stress.....	13
APPENDIX B: Log-linear shape distribution.....	13
7. LITERATURE .....	13

# A Bingham material mixed with stiff particles

## *some theoretical aspects*

Lauge Fuglsang Nielsen  
Department of Civil Engineering  
Technical University of Denmark  
DK-2800 Lyngby, Denmark  
e-mail: lfn@byg.dtu.dk

**Abstract:** A method is developed by which the well-known Bingham description of flow in homogeneous liquids with yield strength is generalized to apply also for composite Bingham materials. In the present context such materials are defined as Bingham materials mixed with very stiff particles of known shape distributions. Various types of shape distributions are considered. In this context, the significance/importance of shape detections in practice is emphasized..

In building materials technology such an analysis is of relevance for the description of fresh self-compacting concretes (SCC). In a special section of the paper some potentials of the theory developed are demonstrated on some aspects of materials design of SCC.

**Key words:** Bingham, Composite Bingham, Shape distribution, Self-compacting concrete (SCC).

## 1. INTRODUCTION

The paper presents a method by which the well-known Bingham description of flow in homogeneous liquids with yield stress can be generalised to apply also for composite Bingham materials. In the present context such materials are defined as traditional Bingham materials, mixed with very stiff particles of known shape distributions. In practice the composite aspects of a generalised Bingham description is a major advantage. Only a few parameters are needed to describe the Bingham behaviour at any composition of the composite considered. Bingham methods normally used need experimental calibration for any new composition.

The analysis performed in this paper is an improved version of an analysis previously made by the author in (1,2). A software, SCC-07, handling most mathematical operations performed in the paper is available on special request to the author.

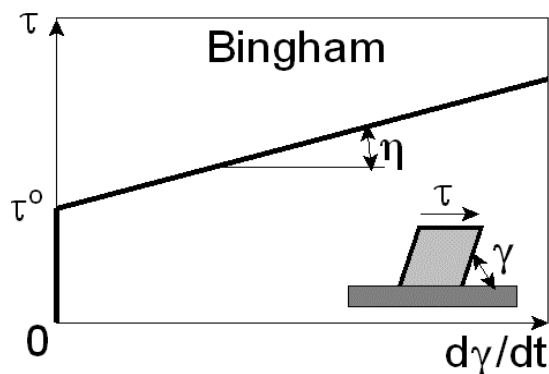


**Figure 1.** Behavior of a Bingham material.  $\tau$  is shear stress.  $\tau^0$  is yield stress, and  $\eta$  is viscosity.  $\gamma$  is angle of deformation.

## 2. BINGHAM MATERIAL

Equation 1, illustrated in Figure 1, describes the constitutive equation for a Bingham material (3,4). It performs as a liquid with viscosity,  $\eta$ , as soon as the shear stress subjected,  $\tau$ , exceeds a yield stress of  $\tau^0$ . Before that it behaves as a rigid solid, which we may think of as an ideal stiff elastic-plastic material with a yield stress,  $\tau^0$ . The angle of deformation is denoted with  $\gamma$ . The rate of angle deformation is  $d\gamma/dt$ .

Experimentally the Bingham parameters can be determined in a number of ways (5). One of the most common methods is to deduce them<sup>1)</sup> from relations, obtained by the so-called coaxial cylinder rheometer, between torsional moment and rate of revolution.

$$\frac{d\gamma}{dt} = \frac{\tau - \tau^0}{\eta} \quad \text{Bingham material} \quad (1)$$

### 3. COMPOSITE BINGHAM MATERIAL

Figure 2 defines a composite Bingham material. It is a mixture of very stiff and strong, non-flexible particles (P) in a Bingham matrix (S). The volume concentration of particles is defined by Equation 2 where V denotes volume. In general subscripts P and S refer to particle phase and matrix phase S respectively. A complete list of symbols is presented at the end of this paper.

$$c = \frac{V_P}{V_P + V_S} \quad \text{Volume concentration of particles} \quad (2)$$

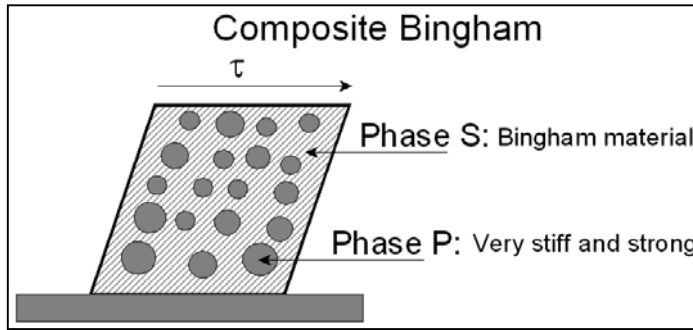


**Figure 2.** Composite Bingham material. The non-flexible particles need not be of spherical shapes.

**Remark:** The term ‘non-flexible’ particles means invariable particle shapes. This is contrary to a general composite geometry, see Figure 3, where phase geometries adapt to each other at any concentration without leaving voids. In the present study, only concentrations  $c \leq c_S$  are considered relevant<sup>2)</sup>.

#### Phase geometry and shape functions

According to a phase-geometrical concept for composites introduced in (6) the phase geometry of composite materials can be described by the shape functions  $(\mu_P, \mu_S)$  outlined in Figure 3, with reference to the geometrical parameters, shape factors  $(\mu_P^0, \mu_S^0)$  and critical concentrations  $(c_P, c_S)$ .

The shape functions for a particulate composite with non-flexible particles (such as Bingham composites) can be written as follows (6).

$$\mu_P = \begin{cases} \mu_P^0 \left(1 - \frac{c}{c_P}\right) & \text{for } c \leq c_S \\ \mu_P^0 \left(1 - \frac{c_S}{c_P}\right) & \text{for } c > c_S \end{cases} ; \quad \mu_S = \begin{cases} \mu_S^0 \left(1 - \frac{c}{c_S}\right) & \text{for } c \leq c_S \\ 0 & \text{for } c > c_S \end{cases} ; \quad c_P = -\frac{\mu_P^0}{\mu_S^0} c_S \quad (3)$$

1) A computer program for such deductions can be found in software ‘Selfcompact’ to be downloaded from <http://www.mat-mek.dk/> (L. Fuglsang Nielsen).

2) For curiosity, extended studies involving  $c > c_S$  (where voids turn up) can be made by a method presented in (6).

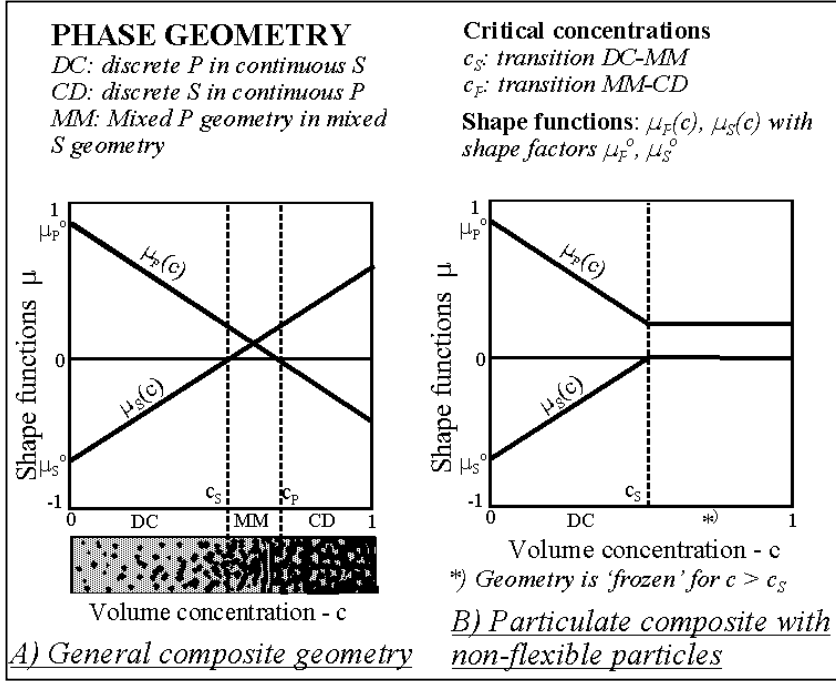


**Figure 3.** A) Composite geometry in general with flexible phase geometries – and B) Particulate composite with non-flexible particles.

## Critical concentrations

We notice from Figure 3 that the critical concentration  $c_S$  is that concentration where well graded phase P particles first interfere and start forming a continuous phase.  $c_S$  can also be thought of as the concentration of the solid phase in a well-packed pile of particles. Subsequently  $c_S$  is also named interference concentration. The critical concentration  $c_P$  is a dependent quantity to be derived from the other geo-parameters as shown in Equation 3.

SHAPE FACTORS	
$\mu_P^0 = \langle m_0 \rangle; \quad \mu_S^0 = -\langle m_\infty \rangle \frac{1 - \langle m_0 \rangle}{1 - \langle m_\infty \rangle}$	
Discrete shape distribution	
$\frac{1}{\langle m_j \rangle} = \sum_{i=1}^{\infty} \frac{\alpha_i}{m_{j,i}} \quad (j = 0, \infty)$ <p><math>\alpha_i</math> is volume fraction of joining aspect ratio <math>A_i</math></p>	
Continuous shape distribution	
$\frac{1}{\langle m_j \rangle} = \int_0^{\infty} \frac{1}{m_j} d\Phi(A) \quad ; \quad (j = 0, \infty)$	
$m_0 = \begin{cases} \frac{3A}{A^2 + A + 1} & (A \leq 1) \\ \frac{3}{4A^2 - 5A + 4} & (A > 1) \end{cases} ; \quad m_\infty = \frac{3A}{A^2 + A + 1} \quad (\text{any } A)$	

**Table 1.** Determination of shape factors when particles have discrete or continuous shape distributions,  $\Phi$ . The aspect ratio is defined by  $A = \text{length/diameter}$  of particles: Spheres (compacts) have  $A = 1$ , long particles have  $A > 1$ , and flat particles have  $A < 1$ . The auxiliary quantities ‘m’ are so-called shape parameters explained in (6).

## Shape factors

Shape factors can be determined from Table 1 based on theories developed in (6). The aspect ratio is defined by  $A = \text{length/diameter}$  of particles: Spheres (compacts) have  $A = 1$ , long particles have  $A > 1$ , and flat particles have  $A < 1$ . Theoretically the term aspect ratio refers to an ellipsoidal particle. Practically it refers to aggregates ‘smoothend’ out to have ellipsoidal shapes.

It is emphasized that the terms, uni- and multi-shaped particles, subsequently used mean mixtures of particles with equal shapes (aspect ratios) and mixtures of particles with various shapes respectively. They *do not refer to size* of particles.

### Uni-shape mixture

For uni-shaped particles the shape factors determined by Table 1 reduces as presented in Equation 4, graphically represented in Figure 4.

$$\mu_P^o = \begin{cases} \frac{3A}{A^2 + A + 1} & A \leq 1 \\ 3 \frac{A^2 - A + 1}{4A^2 - 5A + 4} & A > 1 \end{cases} ; \quad \mu_S^o = \begin{cases} \mu_P^o & A \leq 1 \\ 4\mu_P^o - 3 & A > 1 \end{cases} \quad \text{mixture of uni-shaped particles} \quad (4)$$

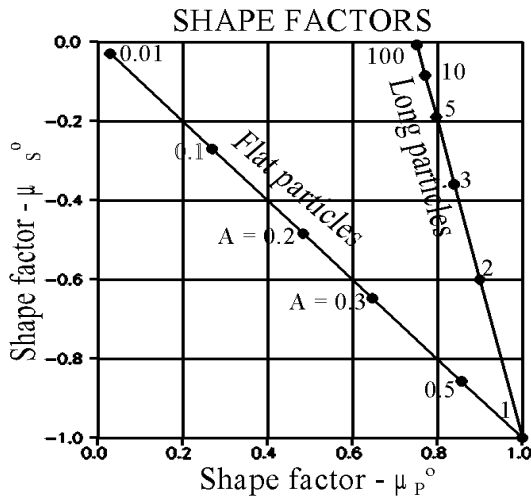
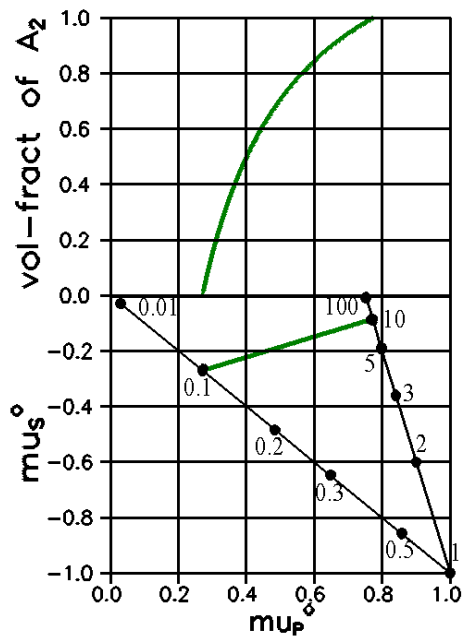


**Figure 4.** Shape factors for uni-shaped particles. (Equation 4).

### Multi-shape mixture



The most simple multi-shaped mixture is the so-called ‘double-shape mixture’ consisting of one group of uni-shaped particles mixed with another group of uni-shaped particles. This mixture can be considered directly by Table 1, section ‘discrete shape distribution’.

An example: We have two sets of aggregates – one set with aspect ratios  $A_1$ , and the other set with aspect ratios  $A_2$ . How do the shape factors change with aggregate compositions. The answer is presented in Figure 5 for a mixture with  $A_1 = 0.1$  and  $A_2 = 10$ . The volume fraction of aggregates with aspect ratio  $A_2$  is presented in the

**Figure 5.** Shape factors for a double-shape mixture made with aggregate ratios  $A_1$  and  $A_2$ . Upper heavy line is volume fraction of particles with  $A_2$ . Associated shape factors are given by the lower heavy line.

upper part of Figure 5. An example is:  $(\mu_P^0, \mu_S^0) = (0.4, -0.22)$  for a 50-50% mixture of the aggregates applied

The more general mixtures are made with continuously shape-distributed particles. A convenient distribution is presented in Equation 5 with applications demonstrated in Figures 6 and 7, where Table 1 has been used to predict shape factors.

#### Arc-tangent shape distribution

$$\Phi = \frac{2}{\pi} \arctan \left( \frac{A}{A_{AV}} \right)^{\pi/s} \quad (A_{AV} \text{ is average, } s \text{ is standard deviation}) \quad (5)$$

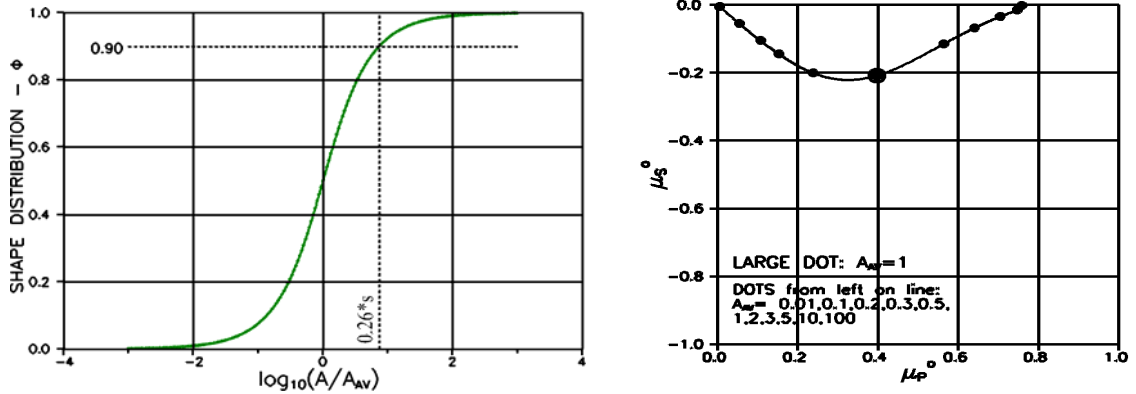


**Figure 6. Left:** Arc-tangent shape distribution with standard deviation  $s = 3.4$  for an aggregate mixture with average aspect ratio,  $A_{AV}$ . Notice that 80% of particles have  $0.13 < A/A_{AV} < 7.7$ . **Right:** Shape factors for such mixtures with various  $A_{AV}$ .

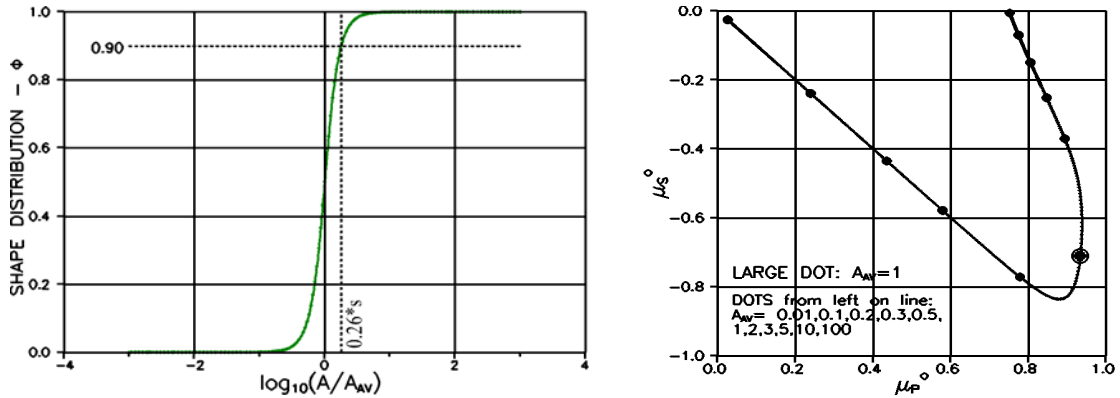


**Figure 7. Left:** Arc-tangent shape distribution with standard deviation  $s = 1.0$  for an aggregate mixture with average aspect ratio,  $A_{AV}$ . Notice that 80% of particles have  $0.56 < A/A_{AV} < 1.78$ . **Right:** Shape factors for such mixtures with various  $A_{AV}$ .

It is emphasized that shape distributions with a standard deviation of  $s$  are considered in general (for any shape average) by Equation 5. An example from Figure 6, right figure: With  $A_{AV} = 1$  the shape factors for a mixture are  $(\mu_P^0, \mu_S^0) \approx (0.4, -0.21)$ , which, incidentally, are similar to the values predicted by Figure 5. With  $A_{AV} = 3$  shape factors are  $(\mu_P^0, \mu_S^0) \approx (0.67, -0.07)$ .

The significance of standard deviations on shape distributions is demonstrated comparing Figure 6 and 7. It is noticed, as expected, that narrower shape distributions (smaller  $s$ ) produce shape factors approaching those predicted in Figure 4 for uni-shaped mixtures.

**Remark:** Another appropriate continuous shape distribution, the so-called log-linear distribution, is demonstrated in Appendix B.

## 4. COMPOSITE PROPERTIES

With known interference concentration ( $c_s$ ) and shape factors ( $\mu_P^0, \mu_S^0$ ) predicted by Table 1, shape functions for a composite Bingham can now be calculated by Equation 3.

### Viscosity

Then composite viscosity can be determined as shown in Equation 5 reproduced from Appendix A at the end of this paper.

$$\begin{aligned} &\text{Arbitrary concentration} \\ &\frac{\eta}{\eta_S} = \frac{1 + c\theta_g^\infty}{1 - c} \quad \text{with} \quad \theta_g^\infty = \begin{cases} \frac{3}{2} \frac{\mu_P + \mu_S - 1}{\mu_S} & c < c_s \\ \infty & c > c_s \end{cases} \\ &\text{Dilute composite (very small concentration)} \\ &\frac{\eta}{\eta_S} = 1 + c(1 + \vartheta_g^\infty) \quad \text{with} \quad \vartheta_g^\infty = \frac{3}{2} \frac{\mu_P^0 + \mu_S^0 - 1}{\mu_S^0} \end{aligned} \quad (5)$$

The relative viscosity predicted for dilute solutions by Equation 5 agrees with Equation 6, first expression, developed by Einstein (7) in his study of the viscosity of dilute sugar solutions. (Spheres have  $A = 1 \Rightarrow (\mu_P^0, \mu_S^0) = (1, -1) \Rightarrow \vartheta_g^\infty = 1.5$ ).

The more general prediction of viscosity by Equation 5 agrees with data obtained from experiments on mixtures made of fluids with finite particle concentrations. Two empirical descriptions (Eilers and Brinkman) for such data are presented in Equation 6 reproduced from (8,9). In Figure 8 these results are compared graphically with the results obtained by the present theory. ( $A = 1 \Rightarrow (\mu_P^0, \mu_S^0) = (1, -1)$  - and  $c_s = 0.78$  estimated from the Eilers expression for  $\eta/\eta_S = \infty$ ).

$$\frac{\eta}{\eta_S} = \left\{ \begin{array}{ll} 1 + 2.5c & \text{Einstein (accurate dilute)} \\ \left( 1 + \frac{1.25c}{1 - 1.28c} \right)^2 & \text{Eilers (empirical)} \\ (1 - c)^{3/2} & \text{Brinkman (empirical)} \end{array} \right\} \quad \text{spherical particles} \quad (6)$$

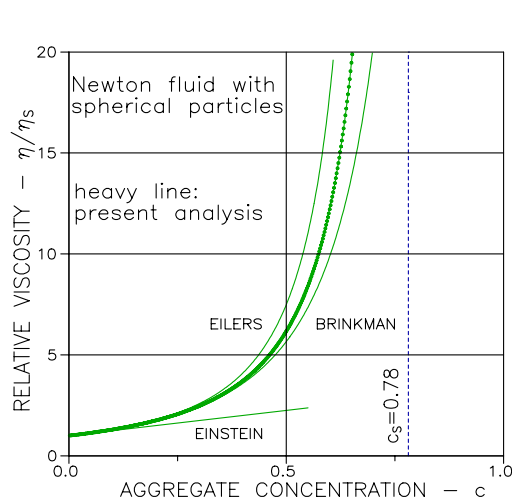


**Figure 8.** Spherical particles ( $A = 1$ ) in a viscous matrix.

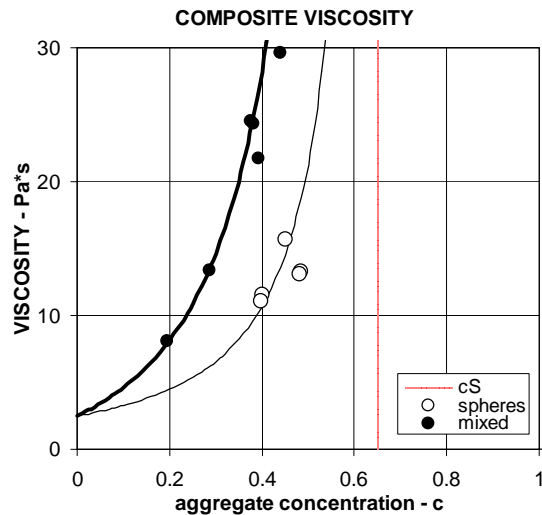


**Figure 9.** Viscosity of concrete as related to fraction of coarse aggregates. Further details are explained in the main text

The experimental results shown in Figure 9 are from tests presented in (1,10). Concretes with various amounts of coarse aggregates were tested at an age of 15 minutes in a coaxial cylinder



rheometer (ConTec BML viscometer). Identical mortars were used in all concretes. Two coarse aggregate types were used: 1) Glass spheres and 2) a mix of 30% sea dredged and 70% crushed aggregates (typical Danish coarse aggregate). Both types of aggregates have an interference concentration of  $c_S \approx 0.65$ .

As before, spheres have an aspect ratio of  $A = 1 \Rightarrow (\mu_P^o, \mu_S^o) = (1, -1)$ . The average shape factors for the mixed aggregates are estimated to be  $(\mu_P^o, \mu_S^o) = (0.40, -0.22)$  from assuming a 50-50% mixture of aggregates with aspect ratios of  $A_1 = 0.1$  and  $A_2 = 10$ , see Figure 5. A mortar viscosity of  $\eta_S = 2.5 \text{ Pa}\cdot\text{s}$  has been estimated.

**Remark:** A complete investigation of aspect ratios was not made in (1). The few measurements/estimates made tell that any  $A > 1$ , which is very un-likely to fully characterize the geometry of natural aggregates. In the author's opinion some 'symmetry' around  $A \approx 1$  must appear in shape-distributions for such particles. The very simple assumption (50-50%) made above reflects this idea – it does not, however, pretend to tell the truth. An arc-tangent distribution predicts similar shape factors when the average aspect ratio is  $A_{AV} = 1$ , see Figure 6.

## Yield stress

According to Equation A4 in Appendix A at the end of this paper a yield stress solution is,

$$\frac{\tau^o}{\tau_S^o} = 1 + c\theta_g^\infty \quad (7)$$

It is hereby assumed that the Bingham material behaves as an elastic matrix with extremely stiff particles until a matrix shear stress of  $\tau_S^o$  is obtained. In other words: The composite starts flowing when phase S starts flowing.

### Pre-flow geometry

Equation 7 presumes a particle phase geometry just as it is when the Bingham material is flowing according to Equation 5. For a number of reasons we cannot be sure that this assumption holds. More or less the 'pre-flow' geometry is influenced by effects which hold the materials structure in a stable state (here as an elastic solid). Special bounds (such as mechanical/physical/chemical) may have developed between matrix and particles, which have to be broken down before flow appears. Such effects add to the composite geometrical complexity.

Increasing geometrical complexity of a composite is associated with lower (numerically) shape functions (6). We assume that the 'pre-flow' geometry can be determined by modifying the 'flow' geometry (Equation 3) as suggested in Equation 8, first expression. Then the yield stress becomes as expressed by the second expression,

$$\begin{aligned} \bar{\mu}_P &= \mu_P^o \left( \frac{\mu_P}{\mu_P^o} \right)^M & ; & & \bar{\mu}_S &= \mu_S^o \left( \frac{\mu_S}{\mu_S^o} \right)^M & \text{with interaction power } M \approx 3.5 \\ \frac{\tau^o}{\tau_S^o} &= 1 + c\bar{\theta}_g^\infty & \text{with } \bar{\theta}_g^\infty &= \begin{cases} \frac{3}{2} \frac{\bar{\mu}_P + \mu_S - 1}{\bar{\mu}_S} & c < c_S \\ \infty & c > c_S \end{cases} \end{aligned} \quad (8)$$

**Remarks:** It is emphasized that the interaction power  $M$  depends on both phases P and S – in a way which cannot, solely, be explained by normal shape functions. With identical phase S matrixes, the interaction power,  $M$ , probably will have to be calibrated to aggregate types (glass, granite, limestone, etc.). The interaction power indicated in Equation 8 has been determined by calibration to the concrete test results previously referred to (1,10).

It should be mentioned that the assumption of elasticity in the pre-flow state of a Bingham material can be disputed. An assumption of ideal stiff plasticity can also be stated. The present choice has been made in order to get a relatively simple method for determining the yield stress of Bingham composites.

The test results in Figure 10 are from the concrete tests (1,10) previously described. A mortar yield stress of  $\tau_s^0 = 1.0$  Pa has been estimated. The predicted yield stresses in Figure 10 have been obtained by Equation 8 with an interaction power of  $M = 3.5$ , *applying for both types of aggregates considered (glass and mixed)*.

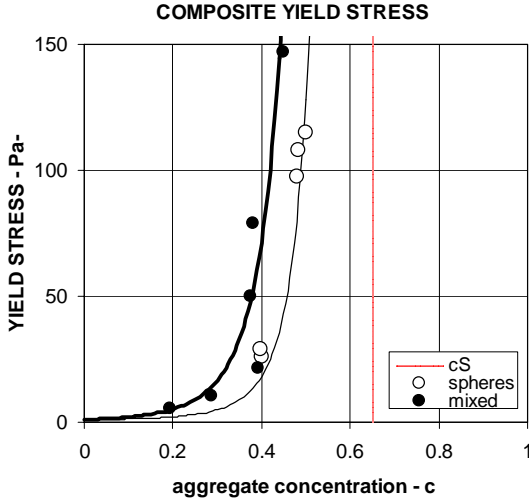


**Figure 10.** Yield strength of concrete as related to fraction of coarse aggregates. Further details are described in the main text.

#### 4. APPLICATION

In this section we will demonstrate some potentials of the theory developed. Self-compacting concretes will be looked at: Which mortar properties must be required in order to develop concretes with prescribed Bingham parameters.

It is emphasized that the analysis made is based on material parameters deduced in this paper. For example, that the pre-flow phase geometry can be characterized by an interaction power of  $M = 3.5$ .

##### Fresh concrete (SCC) versus mortar

In order to work properly, a self-compacting concrete must behave as a Bingham material with properties quantified inside the ‘border lines’ indicated in Figure 11. This suggestion is due to recommendations presented in (11).

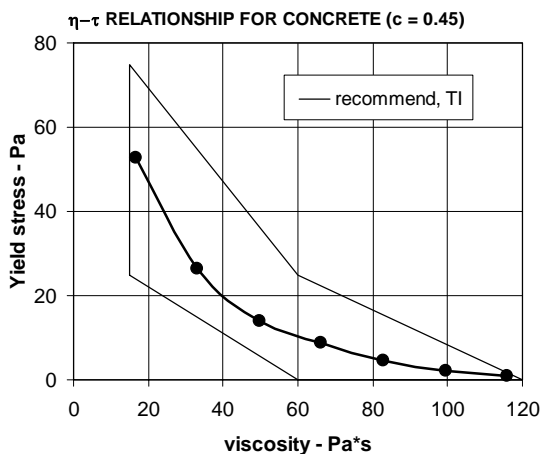


**Figure 11.** Concretes qualified to be self-compacting concretes. A coarse aggregate concentration of  $c = 0.45$  is assumed.

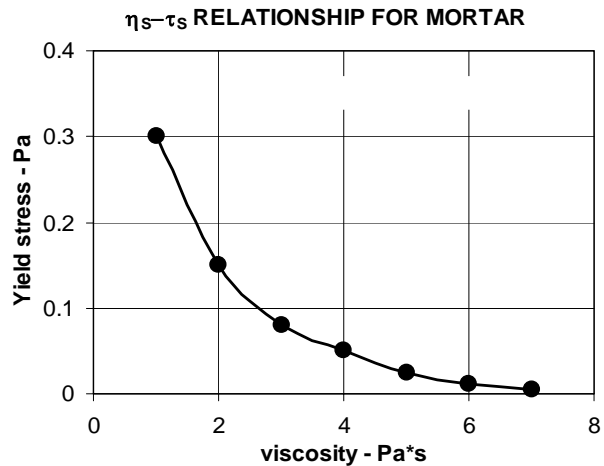


**Figure 12.** Bingham parameters for mortars which can be used for the SCC defined in Figure 11.

We will use the theory developed in this paper to suggest which mortar properties will cause a concrete to follow these recommendations: It is assumed that the concrete considered has a vo-

lume concentration,  $c = 0.45$ , of coarse aggregates similar to the mixed aggregates previously considered ( $(\mu_P^0, \mu_S^0) = (0.40, -0.22)$ ,  $c_S = 0.65$ ).

It is now predicted that mortars to use for the concretes defined in Figure 11 must exhibit Bingham parameters as shown in Figure 12.

**Remark:** A similar procedure can be applied to solve the problem, mortar versus paste, meaning: which paste properties are required in order to develop mortars with prescribed Bingham parameters.

## 5. FINAL REMARKS

The well-known Bingham description of the rheology of homogeneous fluids with yield strength has been generalized in this paper also to include the rheological description of composite Bingham materials. For practice the advantage of such generalization is obvious: The Bingham behavior of composite Bingham materials can be described at any composition from knowing the Bingham properties of the matrix. The traditional composite Bingham descriptions need experimental calibration at any new composition.

The geometry of the aggregate phase is considered in the theory by so-called shape functions with shape factors determined from shape distributions. Various appropriate types of such distributions are considered.

An hypothesis has been made that particle surfaces act differently (more efficiently) in the ‘pre-flow’ and the ‘flow’ states of a composite Bingham material. A materials dependent interaction power,  $M$ , (to be experimentally determined) has been introduced to consider this effect.

*Future research:* Two fields of future research are revealed: 1) The significance of the interaction power,  $M$ , has been explained in Section ‘pre-flow geometry’. The hypothesis suggested has to be stronger justified. 2) The significance/importance of shape distributions has been identified. Methods for practice have to be developed for measuring such distributions.

*A curiosum:* The analysis made in this note on composite Bingham materials with stiff particles can easily be generalized to apply also for composite Bingham materials with soft particles (voids). Only a few obvious modifications have to be introduced (2). This feature might be useful when tailoring the viscosity of composite Bingham materials, for example by modifying the matrix properties by air entrainment.

Application to fresh self-compacting concrete of the theory presented seems worth-while. As such the theory may be considered as an alternative to other methods developed by other authors in the field of SCC - such as in (12,13,14,15,16,17,18).

## 6. NOTATIONS

Abbreviations and subscripts	
V	Volume
P	Phase P
S	Phase S
g	Shear
No subscript	Composite material
Geo-parameters	
$c = V_P/(V_P+V_S)$	Volume concentration of phase P
A	Aspect ratio, length/diameter of ellipsoidal particle
$A_{AV}$	Average aspect ratio
$\phi$	Distribution of aspect ratios
s	Standard deviation
$\mu^0$	Shape factor
$\mu$	Shape function
$c_P, c_S$	Critical concentrations

$\theta, \theta$	Geo-function
$M$	Interaction power
	<b>Stiffness and other properties (shear)</b>
$G$	Stiffness (Shear modulus)
$n_g = G_P/G_S$	Stiffness ratio
$\eta$	Viscosity
$\tau^0$	Yield stress
	<b>Stress (shear)</b>
$\tau$	Shear stress

## APPENDIX A: Analogy

### *Elastic-viscous analogy*

According to the elastic-viscous analogy we can determine solutions to a liquid problem from the elastic counterpart solutions by replacing shear moduli with viscosities, deformations with deformation velocities, and considering stresses as shear stresses ( $\tau$ ).

In the present context we will look at the Bingham liquid problem: Two liquids, phase S with viscosity  $\eta_S$ , and phase P with viscosity  $\eta_P$ , are mixed: How does the composite behave?

### *Elastic composite: shear modulus and phase stresses*

The elastic counterpart problem to solve is: Two elastic materials, phase P with shear modulus  $G_P$ , and phase S with shear modulus  $G_S$ , are mixed. How does the composite behave?

The appropriate elastic solution is the one where Poisson's ratios  $\nu_P = \nu_S = 0.5$  apply, meaning that the phases are incompressible (such as in liquids). The composite solutions for shear modulus and phase stresses are the following developed in (6).

$$\left. \begin{aligned} \frac{G}{G_S} &= \frac{n_g + \theta_g [1 + c(n_g - 1)]}{n_g + \theta_g - c(n_g - 1)} && \text{(Shear modulus)} \\ \frac{\tau_S}{\tau} &= \frac{n_g + \theta_g}{n_g + \theta_g [1 + c(n_g - 1)]} && \text{(Phase S stress)} \\ \frac{\tau_P}{\tau} &= \frac{n_g (1 + \theta_g)}{n_g + \theta_g [1 + c(n_g - 1)]} && \text{(Phase P stress)} \end{aligned} \right\} \begin{array}{l} \text{elastic composite in general} \\ \text{with stiffness ratio } n_g = G_P/G_S \end{array} \quad (A1)$$

For particulate composites with non-flexible particles the composite geometry is considered by the following geo-function ( $\theta_g$ ) with shape functions ( $\mu$ ) introduced from Equation 3, Section 3.

$$\theta_g = \frac{3}{4} \left[ \mu_P + n_g \mu_S + \sqrt{(\mu_P + n_g \mu_S)^2 + 4n_g(1 - \mu_P - \mu_S)} \right] \quad \text{geo-function} \quad (A2)$$

### *Extremely stiff particles*

When phase P is extremely stiff ( $n_g \Rightarrow \infty$ ) Equations A1 and A2 reduce as follows

$$\left. \begin{aligned} \frac{G}{G_S} &= \frac{1 + \theta_g^\infty c}{1 - c} ; \quad \frac{\tau_S}{\tau} = \frac{1}{1 + c\theta_g^\infty} ; \quad \frac{\tau_P}{\tau} = \frac{1 + \theta_g^\infty}{1 + c\theta_g^\infty} \\ \text{with } \theta_g^\infty &= \begin{cases} \frac{3}{2} \frac{\mu_P + \mu_S - 1}{\mu_S} & \text{for } c < c_S \\ \infty & \text{for } c \geq c_S \end{cases} \end{aligned} \right\} \begin{array}{l} \text{Elastic composite} \\ \text{with very stiff particles} \end{array} \quad (A3)$$

### Composite Bingham material: viscosity and stress

Following the elastic-viscous analogy the counterpart viscous solution to Equation A3 is the following Equation A4, expressing the viscosity of, and the phase S stress in the composite liquid considered.

$$\left. \begin{aligned} \frac{\eta}{\eta_S} &= \frac{1 + \theta_g^\infty c}{1 - c} && \text{Viscosity} \\ \frac{\tau_S}{\tau} &= \frac{1}{1 + c\theta_g^\infty} && \text{Phase S stress} \end{aligned} \right\} \text{Liquid with very stiff particles} \quad (A4)$$

**Remark:** We notice that the phase S stress solution applies for both an elastic and a liquid composite. For the composite Bingham material, defined in Sections 2 and 3, this means that this solution applies also in the ‘pre-flow’ state (see Section ‘yield stress’).

### APPENDIX B: Log-linear shape distribution

Shape factors are determined in Section 3 (Table 1) for uni-shaped mixtures, double-shaped mixtures, and mixtures with so-called arc-tangent shape distributions. In this appendix an alternative to the latter distribution is presented in Equation B1, namely the log-linear shape distribution demonstrated in Figure B1.

#### Log-linear shape distribution

$$\phi = \frac{1}{2} \left( 1 + \frac{\log_{10}(A/A_{AV})}{s} \right) \equiv \begin{cases} 0 & \text{when } \log_{10}(A/A_{AV}) < -s \\ 1 & \text{when } \log_{10}(A/A_{AV}) > s \end{cases} \quad (B1)$$

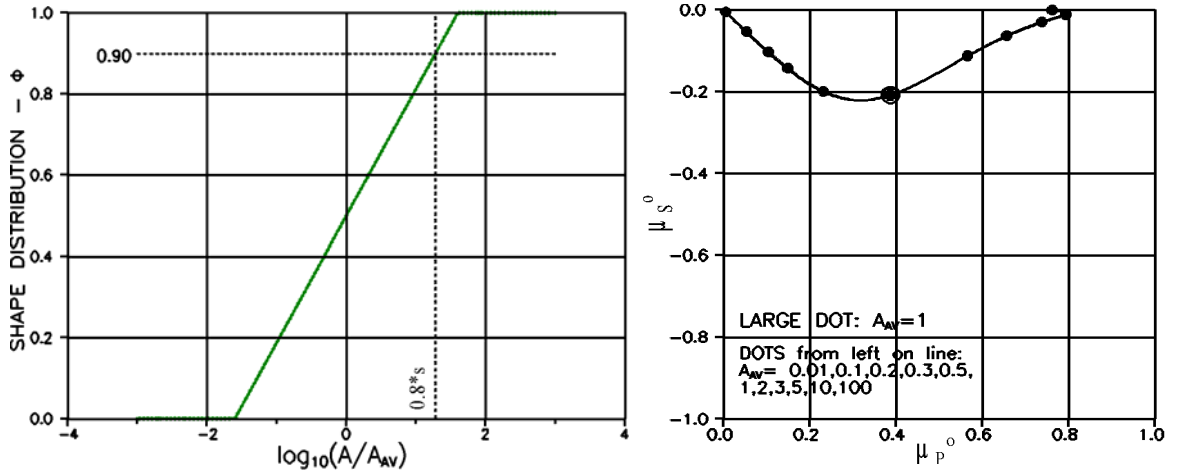


**Figure B1. Left:** Log-linear shape distribution with standard deviation  $s = 1.6$  for an aggregate mixture with average aspect ratio,  $A_{AV}$ . Notice that 80% of particles have  $0.052 < A/A_{AV} < 19.1$ . **Right:** Shape factors for such mixtures with various  $A_{AV}$ .

## 7. LITERATURE

1. Geiker, M.R., Brandl, M., Thrane, L. Nyholm, and Nielsen, L. Fuglsang: "On the effect of coarse aggregate fraction and shape on the rheological properties of self-compacting concrete". ASTM, Cement, Concrete, and Aggregates, 24(2002), No.1.
2. Nielsen, L. Fuglsang: "Rheology of extreme composites", In "Papers in Structural Engineering and Materials - A Centenary Celebration", 179-187, Dept. of Struct. and Materials, Tech. Univ. Denmark, 2000.

- 
3. Bingham, E.C.: "An investigation of the laws of plastic flow", Bur. of Standards Bull., 13(1916), 309. 'Colloid types', Fifth Coll. Symp. Monograph, 1(1928), 219.
  4. Reiner, M.: "Lectures on theoretical rheology" (third edition), North-Holland Publishing Company, Amsterdam, 1960.
  5. Ferraris, C.F.: "Test Methods to Measure the Rheological Properties of High-Performance Concrete: State of the Art report", J. Res. NIST, 104[5], 461-578 (1999).
  6. Nielsen, L. Fuglsang: "Composite Materials – Properties as Influenced by Phase Geometry", Springer Verlag, Berlin, Heidelberg, New York, 2005.
  7. Einstein, A.: "Eine neue Bestimmung der Moleküldimensionen", An. Physik, 19(1906), 289 and 34(1911), 104.
  8. Holliday, L. (ed): "Composite materials", Elsevier Publishing Company, New York, 1966, (p. 34, Chapter on Inclusions in a Viscous Matrix).
  9. Eirich, R.F. (ed): "Rheology, Theory and Applications", Academic Press Inc., New York, 1958, (p. 363, Chapter on Rheological Properties of Asphalt).
  10. Brandl, M. and Thrane, L. Nyholm: "Rheological properties of Self Compacting Concrete (SCC)", M.Sc. thesis, Department of Civil Engineering, Tech. Univ. Denmark, 2001.
  11. Technological Institute, Denmark: "Knowledge about SCC" (Viden om SCC), Information sheet, updated 20.01.2007
  12. Wallevik, O.H.: "The rheology of the fresh concrete and applications for concrete with and without silica fume", Dr.ing. thesis, The Norwegian Institute of Technology – NTH, Norway, 1990.
  13. Ferraris, C.F. and de Larrard, F.: "Testing and modeling of fresh Concrete Rheology", National Institute of Standards and Technology, Washington DC, NIST Report 1094, 1998.
  14. De Larrard, F.: "Concrete Mixtures Proportioning: A Scientific Approach", Modern Concrete Technology Series, E&FN SPON, London 1999.
  15. Oh, S.G., Nogushi, T. and Tomosawa, F.: "Towards mix design for rheology of self-compacting concrete", in proc. of First International RILEM Symposium on Self-Compacting Concrete (eds. Skarendahl, Å. and Peterson, O.), Stockholm, September 13-14, 1999, Proc 7, S.A.R.L., Cachan, 1999, pp. 361-372.
  16. Wüstholtz, T.: "Experimentelle und theoretische Untersuchungen der Frischbetoneigenschaften von Selbstverdichtendem Beton", Dr. thesis, Universität Stuttgart, Institut für Werkstoffe im Bauwesen, 2005.
  17. Wüstholtz, T.: "A model approach to describe the fresh properties of self-compacting concrete (SCC)", Otto-Graf-Journal, Vol. 16, 2005, pp. 79-93.
  18. Westerholm, M.: "Rheology of the Mortar Phase of Concrete with Crushed Aggregate", Ph.D. thesis, Luleå Univ. of Technology, Dept. Chem. Eng. and Geosciences, Division of Mineral Processing, 2006.